Simulation of X-ray in-line phase contrast

M. Langer, Z. Cen, L. Weber, J. M. Letang, S. Rit, F. Peyrin

Université de Lyon, CREATIS ; CNRS UMR 5220 ; Inserm U1044 ; INSA-Lyon ; Université Lyon 1, Villeurbanne, France.

European Synchrotron Radiation Facility, Grenoble, France

max.langer@creatis.insa-lyon.fr

Background

- Aim: Monte Carlo simulation of X-ray in-line phase contrast
  - Infrastructure for grid computing exist (VIP, Gatelab, …)
  - Focus is for the moment on the physics problems
  - Master thesis Zhenjie Cen
  - PhD Loriane Weber

- Outline
  - What is X-ray phase contrast?
  - My focus: Image reconstruction – phase tomography
  - Application – bone imaging
  - Problems – motivation for simulation
  - Developments – Deterministic -> Probabilistic
  - Future work

X-ray phase contrast imaging

- **Acquisition:** Propagation-based imaging, using several distances [2, 3]

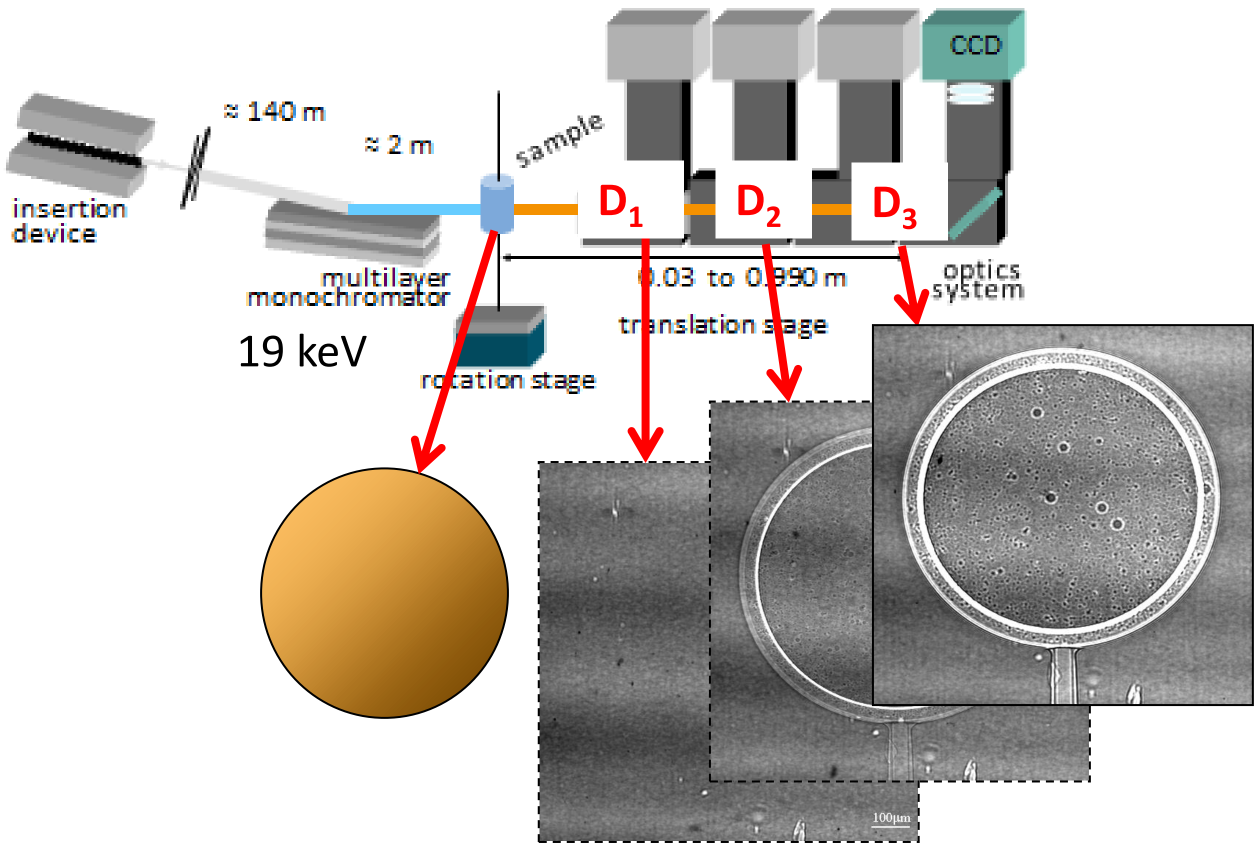

Phase contrast increases with the propagation distance

- High degree of coherence
- Parallel-beam set-up
- Micrometric resolution

[2] Cloetens et al., *Appl. Phys. Lett.*, 1999
[3] Zabler et al., *Rev. Sci. Inst.*, 2005

X-ray phase contrast imaging

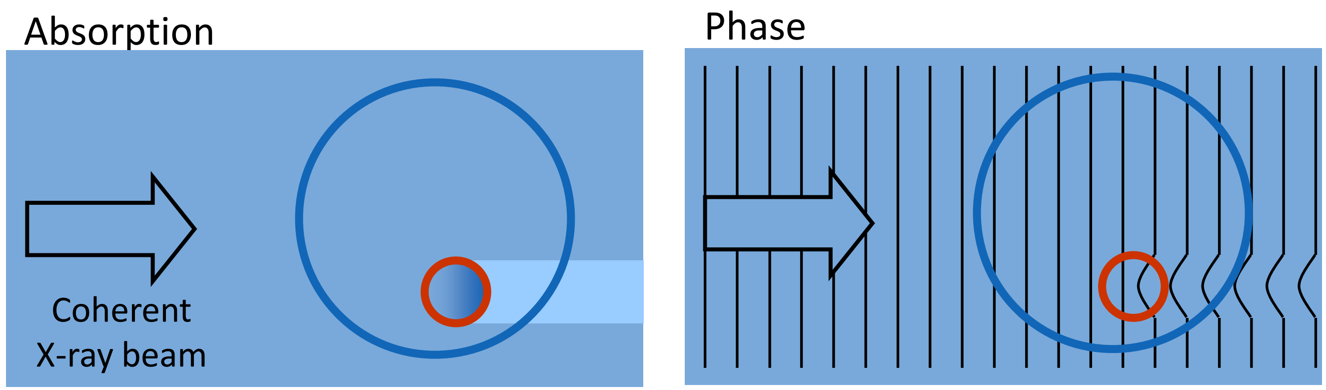

- Refractive index

$$n(x, y, z) = 1 - \delta_n(x, y, z) + i\beta(x, y, z)$$

  - δ_n related to the **phase shift**
  - β related to the **absorption**

- For hard X-rays, $\delta_n/\beta > 10^3$ [2]

  → PCI offers higher sensitivity than attenuation-based imaging.

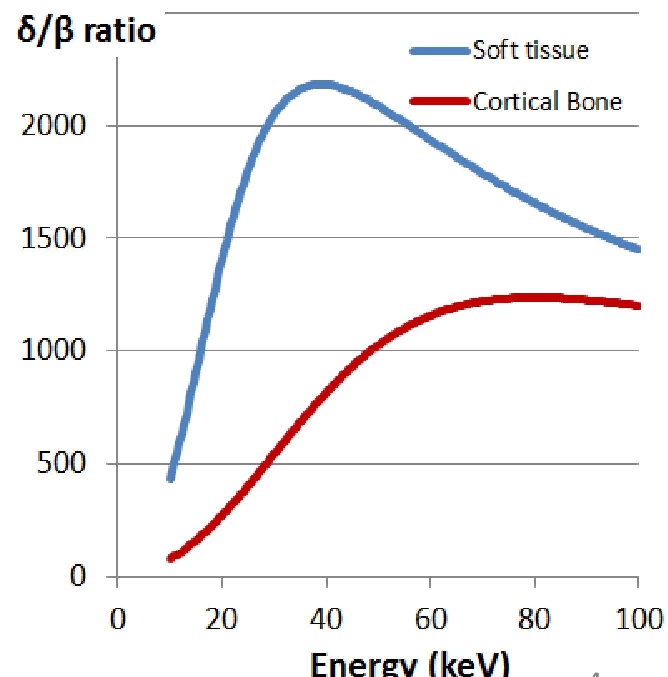

[2] Momose et al., *Nature Medicine*, 1996.

Phase Retrieval

- Quantitative, non-linear relationship between phase shift and contrast

$$I_D(\mathbf{x}) = \left|\mathrm{Fr}_{D,\lambda}[\mathrm{T}_{A,\varphi}(\mathbf{x})]\right|^2$$

- Phase retrieval: inverse problem of calculating phase shift from phase contrast images at different distances

$$\varphi(\mathbf{x}) = \arg\min_{\varphi} \left\| \left|\mathrm{Fr}_{D,\lambda}[\mathrm{T}_{A,\varphi}(\mathbf{x})]\right|^2 - I_D(\mathbf{x}) \right\|^2$$

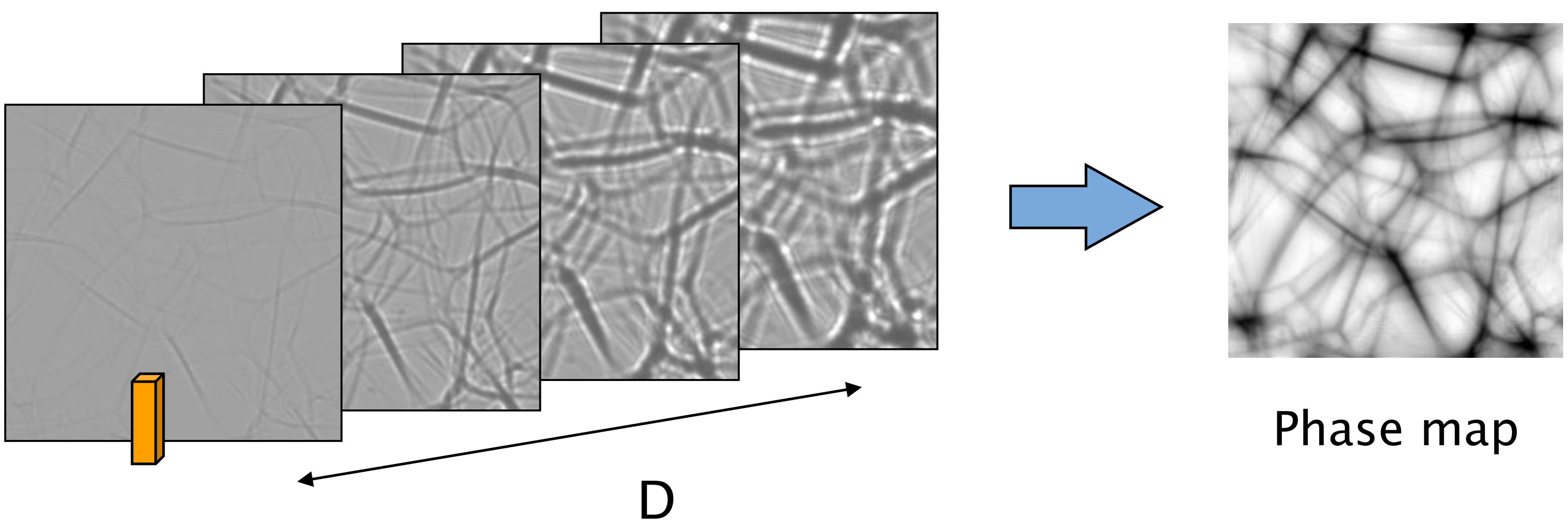

Phase Tomography

- Phase shift is projection through refractive index
- Refractive index can be reconstructed by tomography
- Phase tomography usually divided into a two-step process
  - Phase retrieval (2D)
  - Repeated for each projection angle, tomography (3D)
- Refractive index proportional to electron density
  - I.e. mass density for most materials

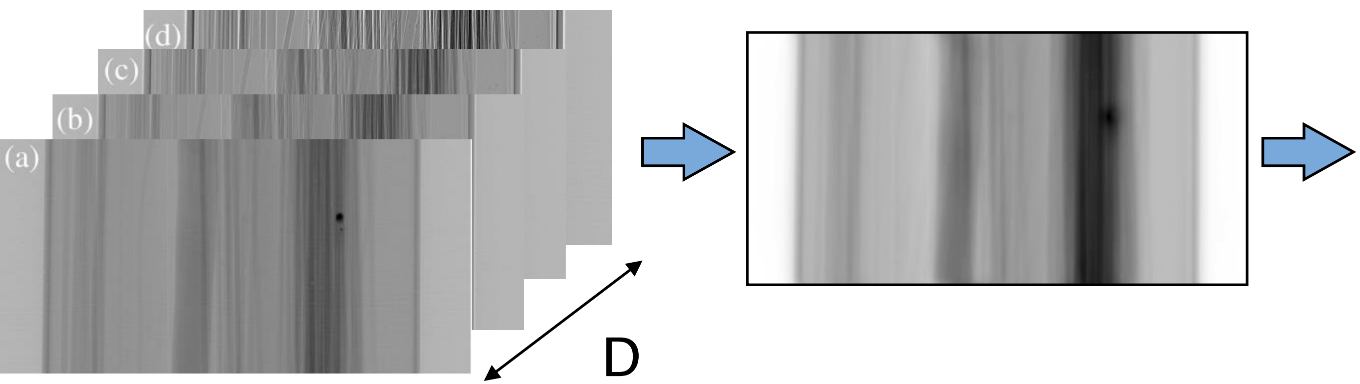

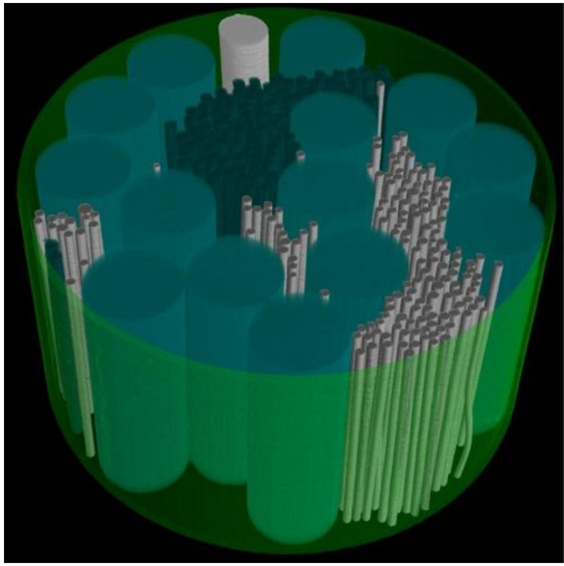

X-ray phase contrast imaging

- Synchrotron Radiation [1]:
  - Intense
  - Stable
  - Coherent

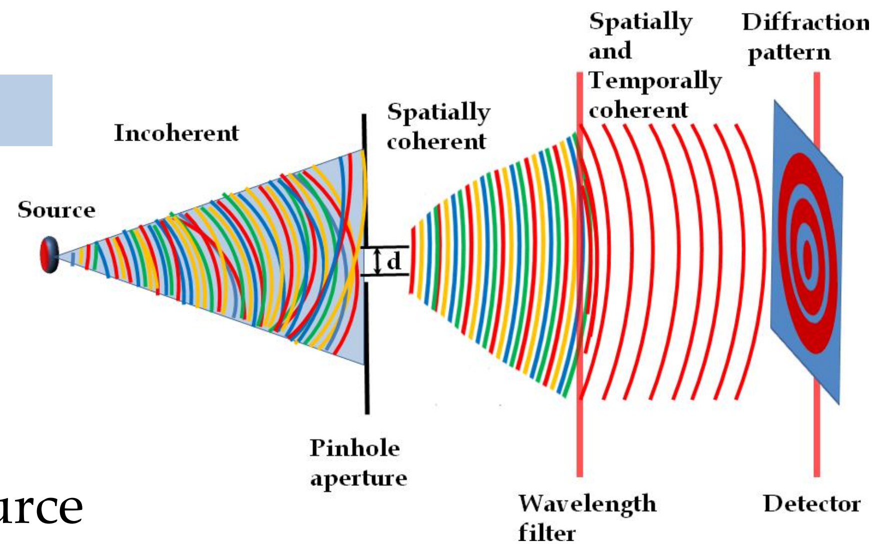

- Coherence
  - Spatial → point-likeness of the source
  - Temporal → monochromaticity

X-ray Phase Nano-Tomography

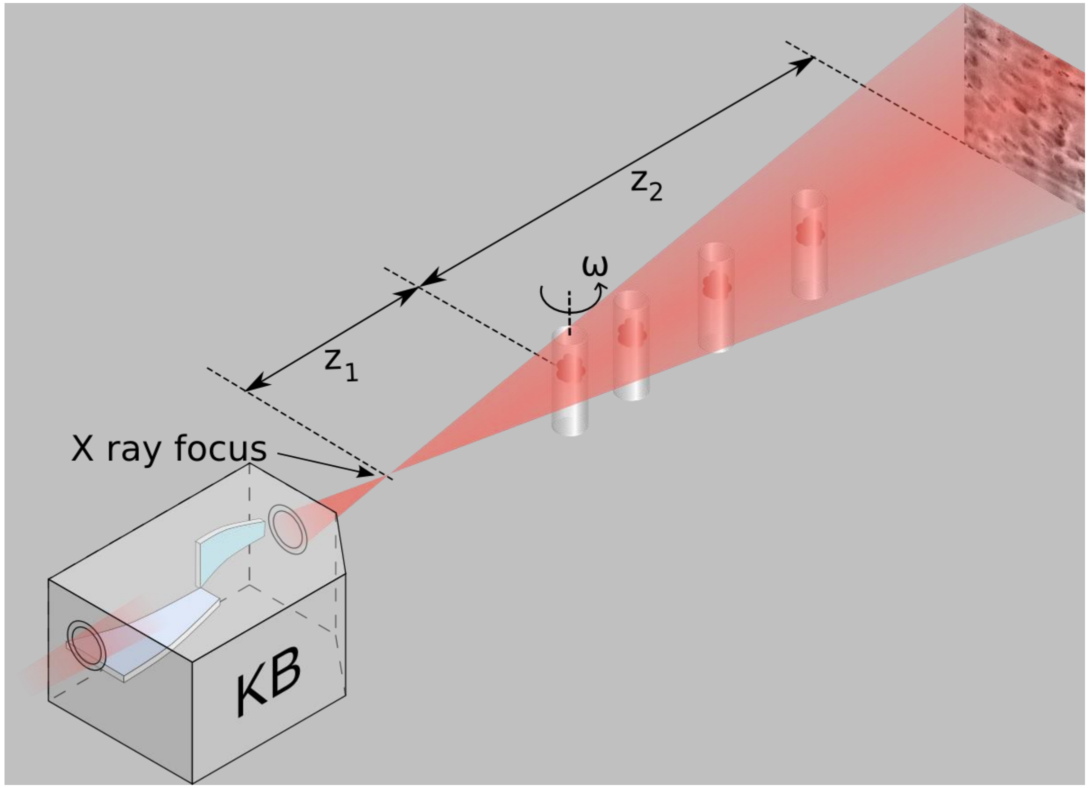

- **Zoom** non-destructively into a region of interest of a tissue, cell, ...
- Ideal for **multi-scale approaches**
- Magnified phase contrast imaging
    - **Quantitative** reconstruction of the **electron density**
    - Very **high sensitivity**
    - High resolution (X-ray wavelength limited)

R Mokso, P Cloetens, E Maire, W Ludwig, JY Buffière, APL, 2007, 90, 144104

Nano-Imaging end-station ID16B

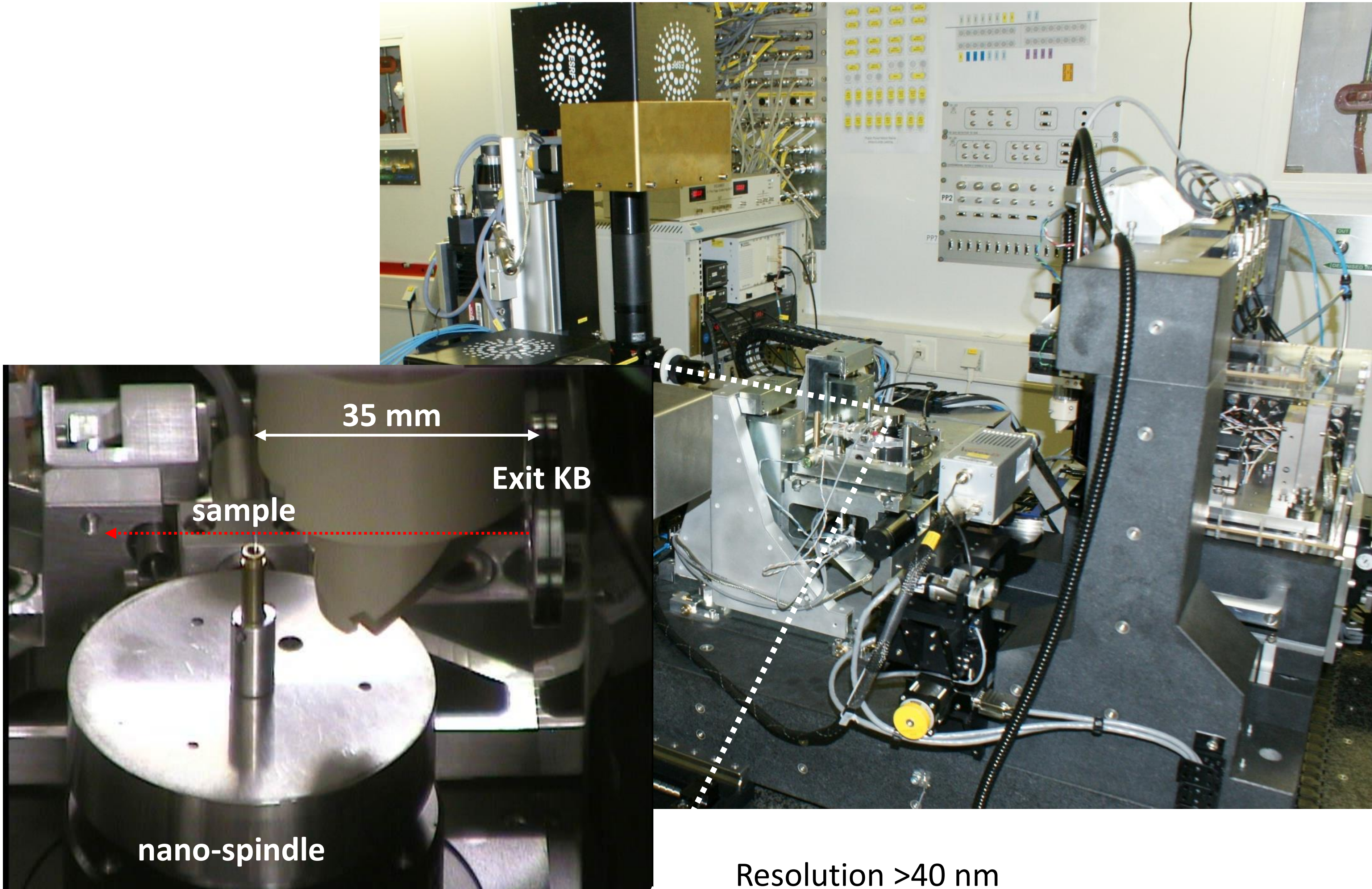

Resolution >40 nm

Nano-imaging end-station ID16A

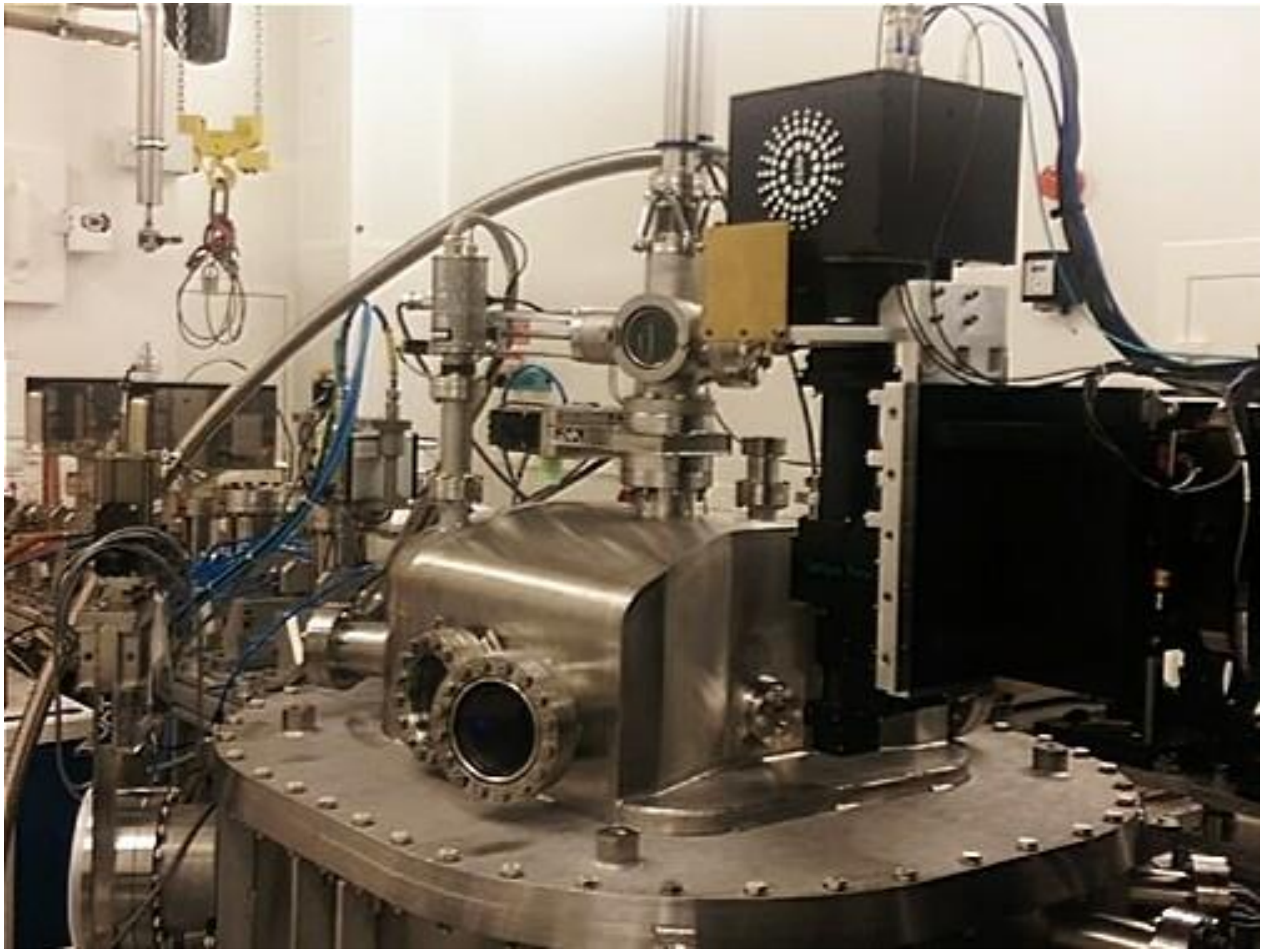

- Imaging in vacuum @ 17 & 33 keV
- Cryo-cooling capability
- Target resolution <20 nm

Projection Microscopy

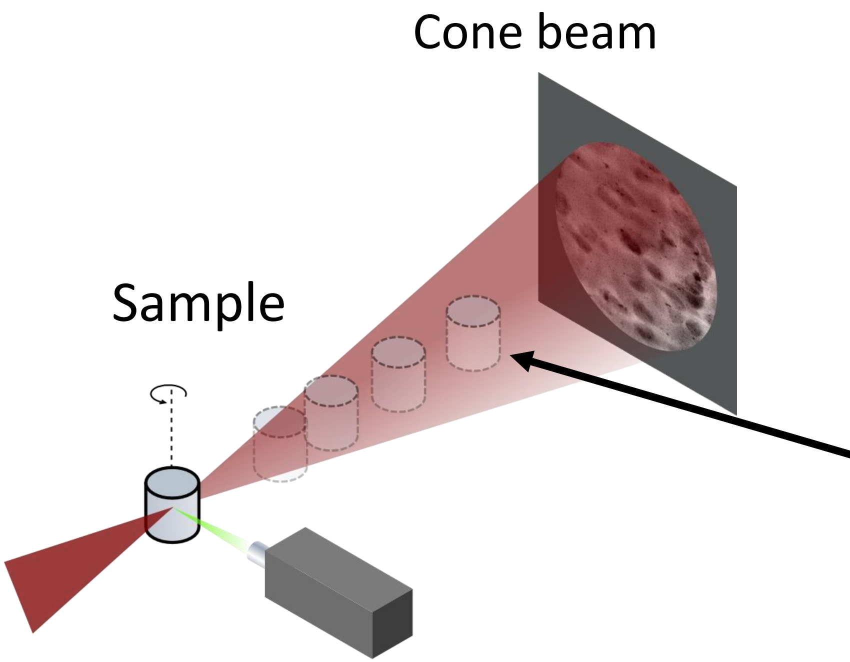

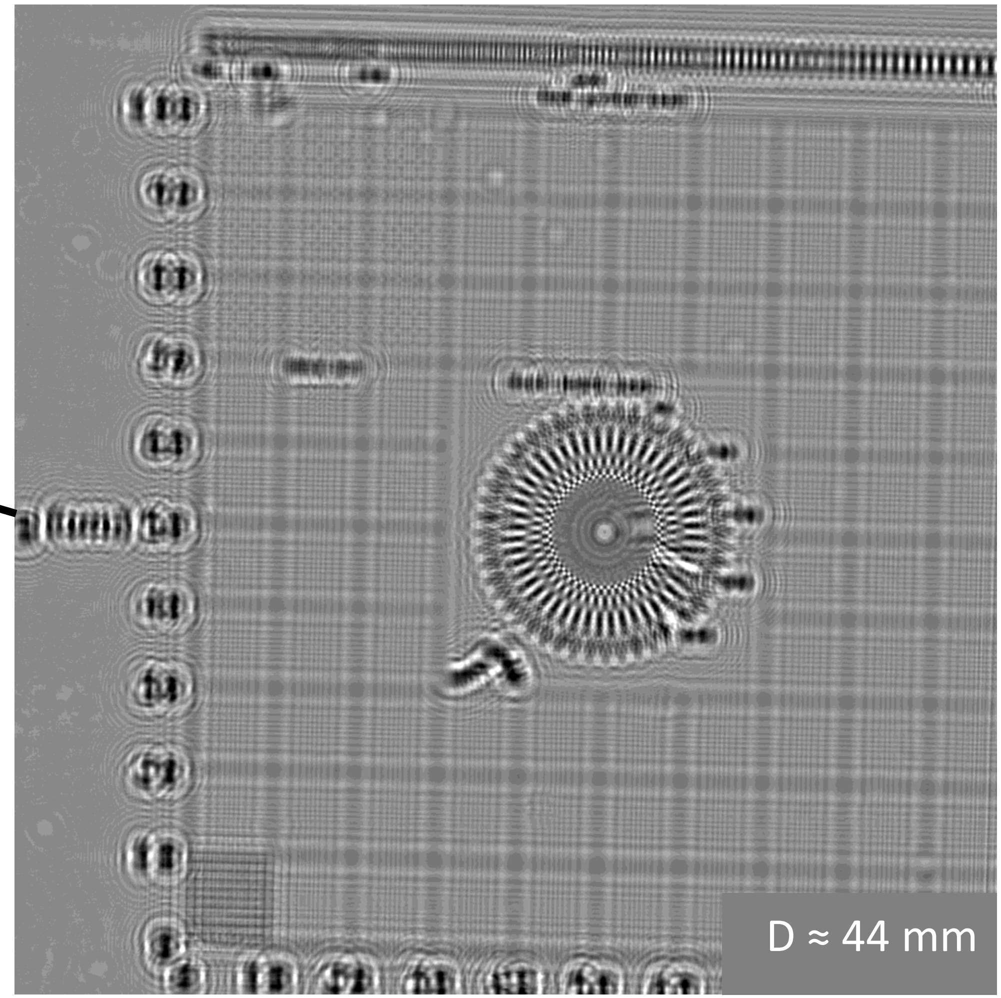

Magnified in-line holograms
of Au Xradia test pattern
E = 17.3 keV

Projection Microscopy

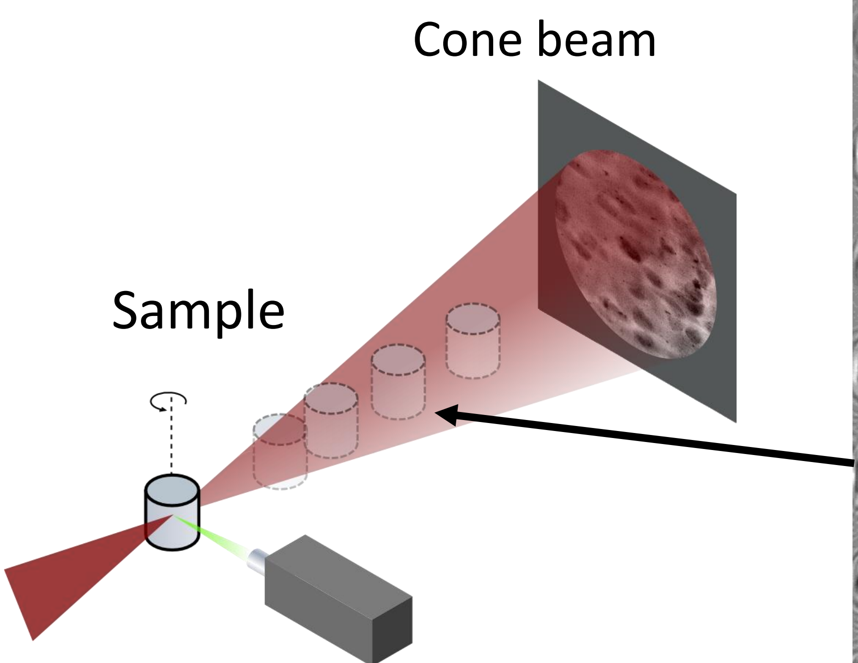

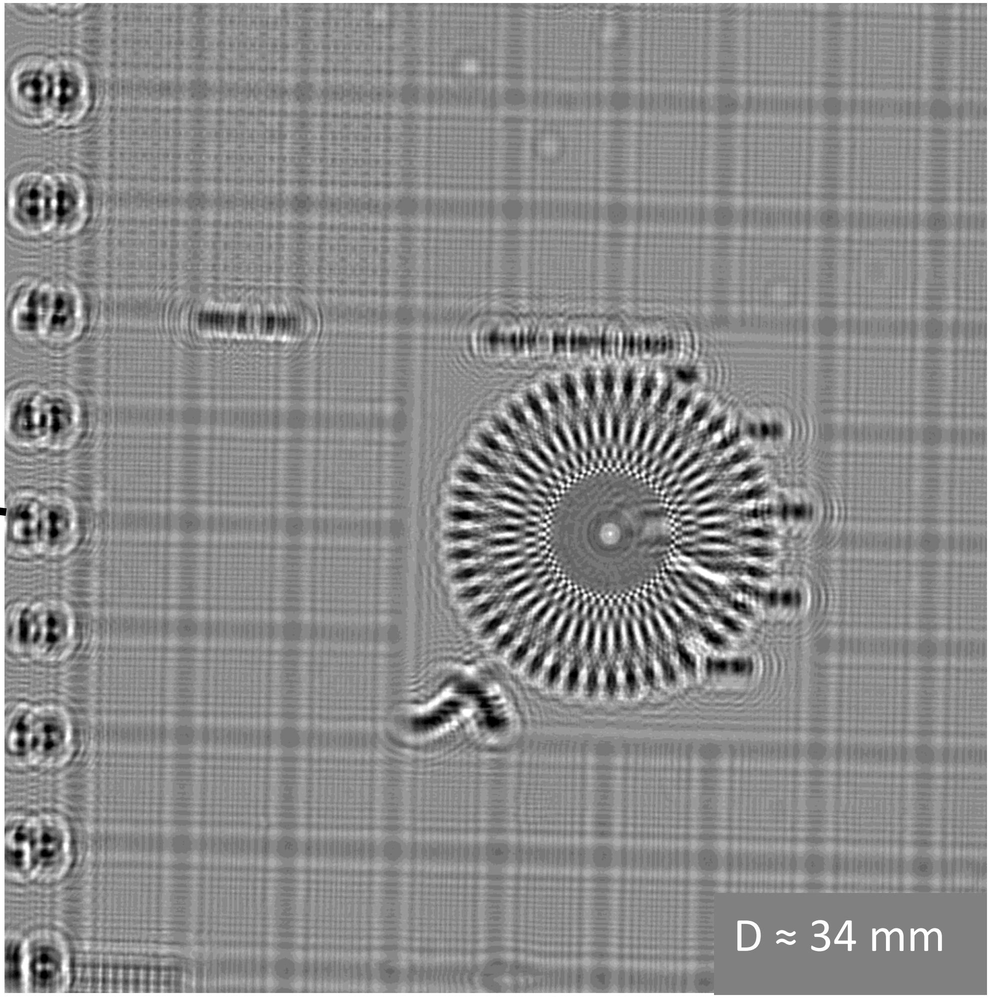

Magnified in-line holograms
of Au Xradia test pattern
E = 17.3 keV

Projection Microscopy

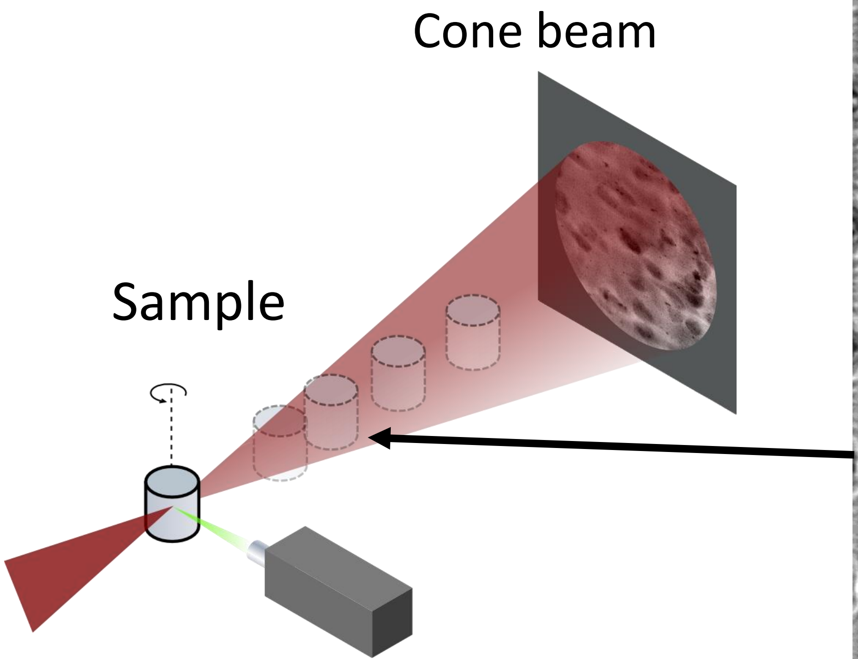

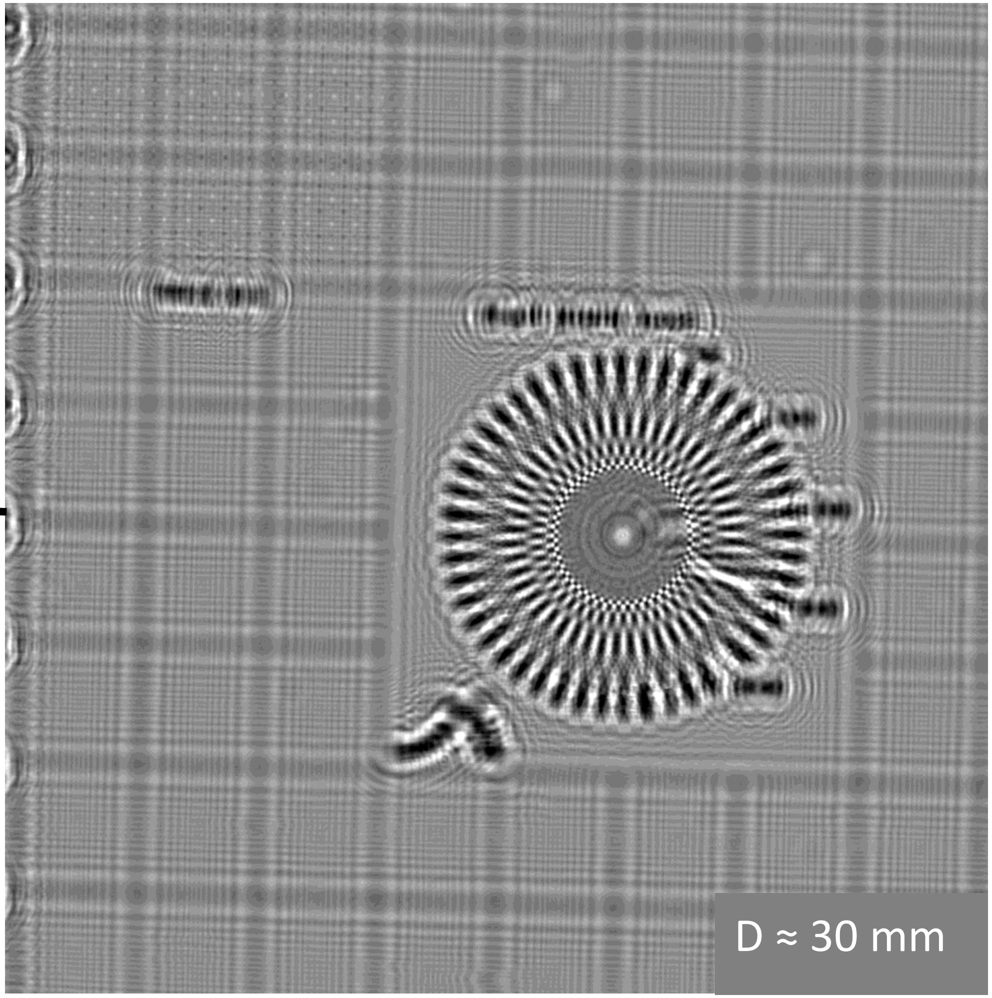

Magnified in-line holograms
of Au Xradia test pattern
E = 17.3 keV

Projection Microscopy

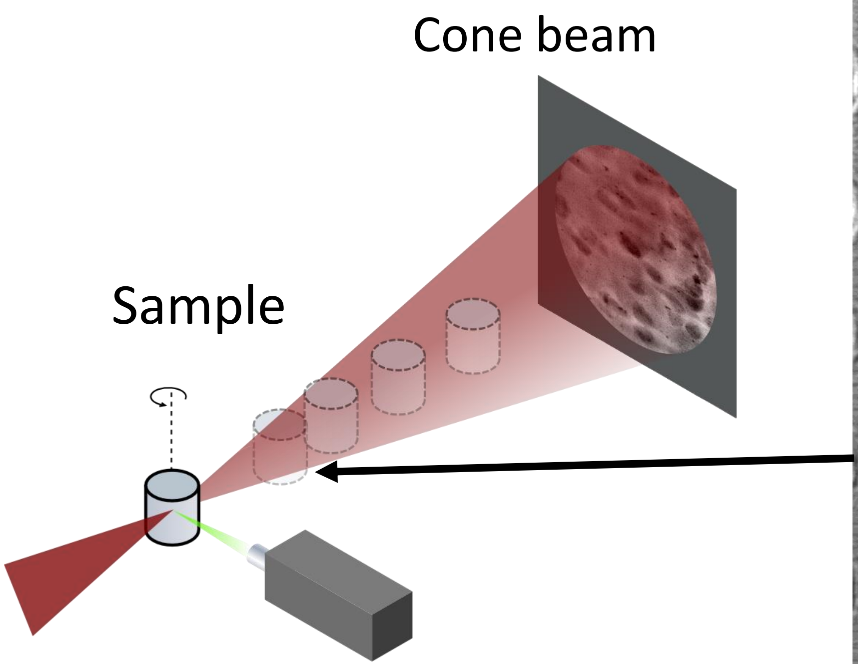

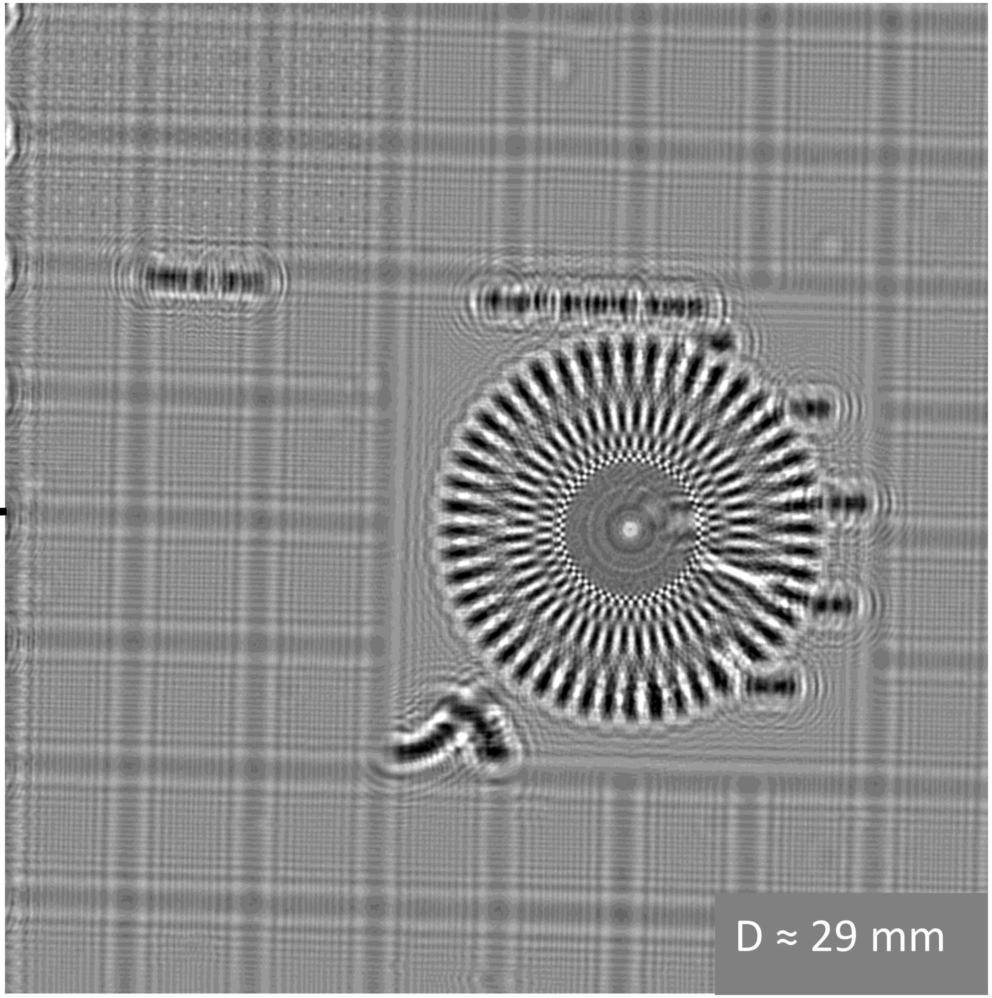

Magnified in-line holograms
of Au Xradia test pattern
E = 17.3 keV

Projection Microscopy: phase retrieval

X-radia gold test pattern
Innermost line width: 50 nm
Energy = 17.3 keV
Field of view: 80 μm
Pixel size: 53 nm

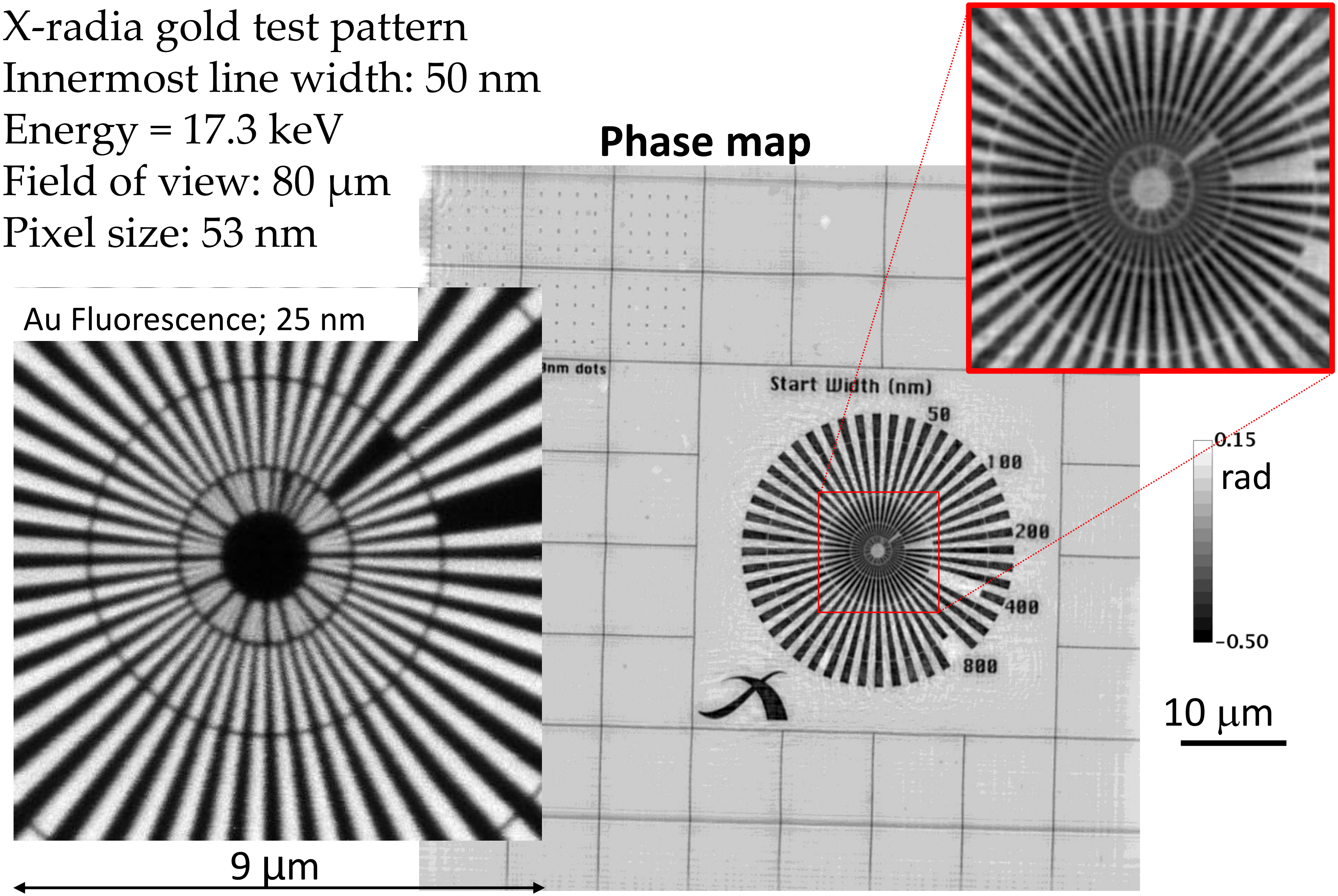

Phase nanotomography of bone

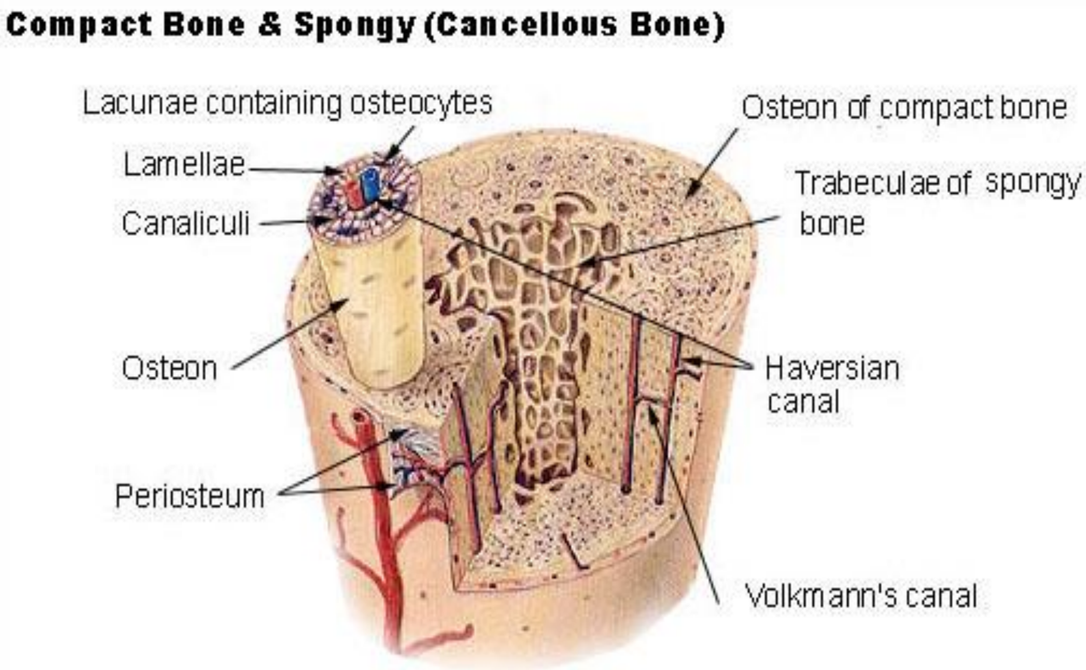

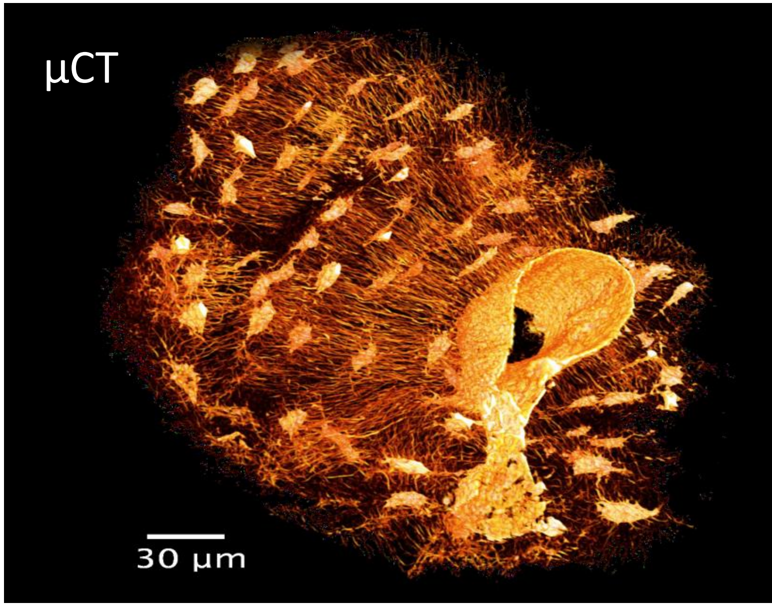

Pacureanu et al., *Med. Phys.* 2012

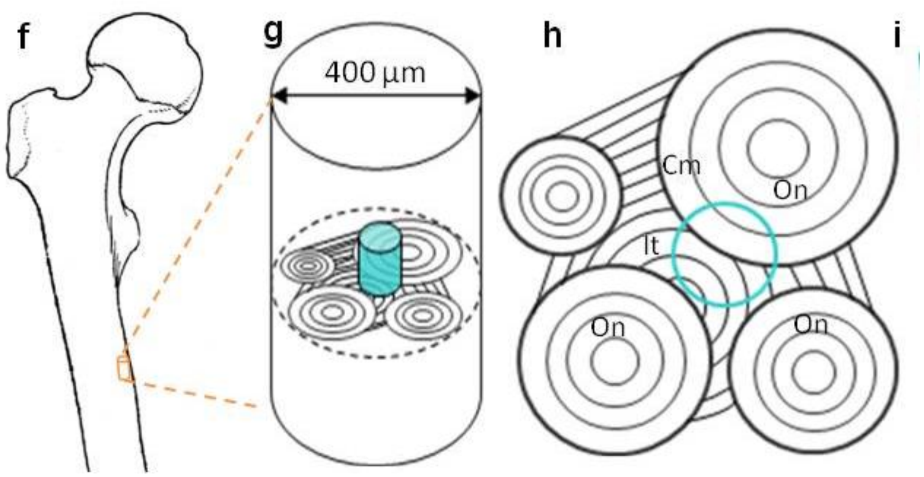

120 µm

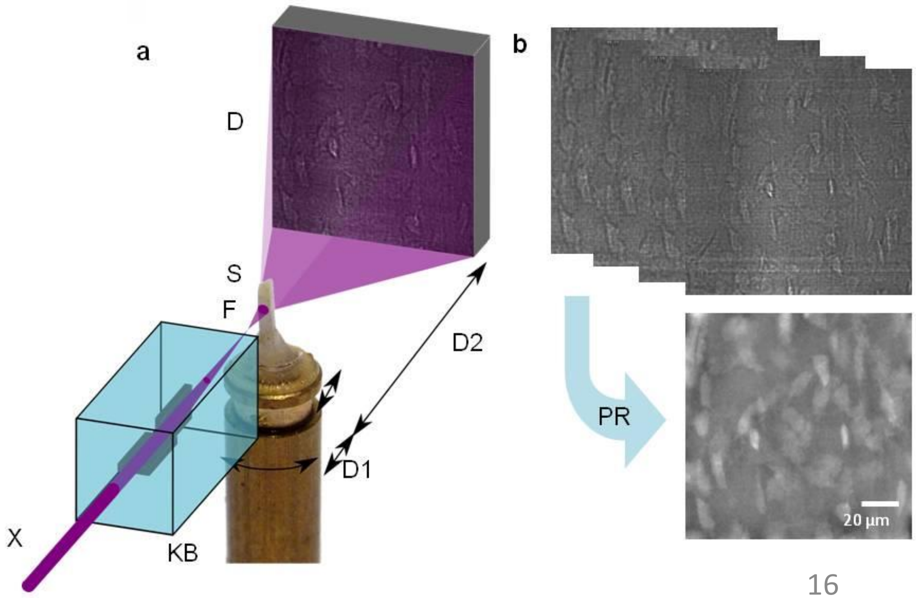

3D reconstruction

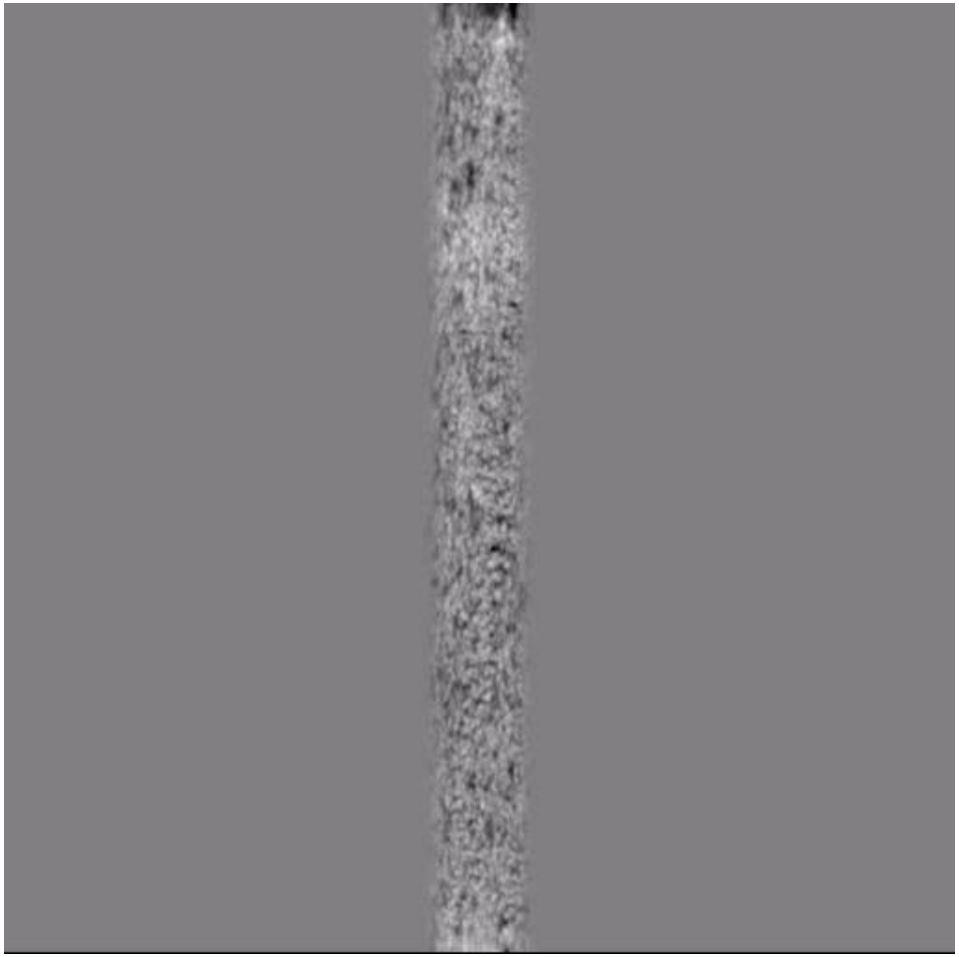

3D volume rendering

Analysis of the Lacuno-Canalicular network

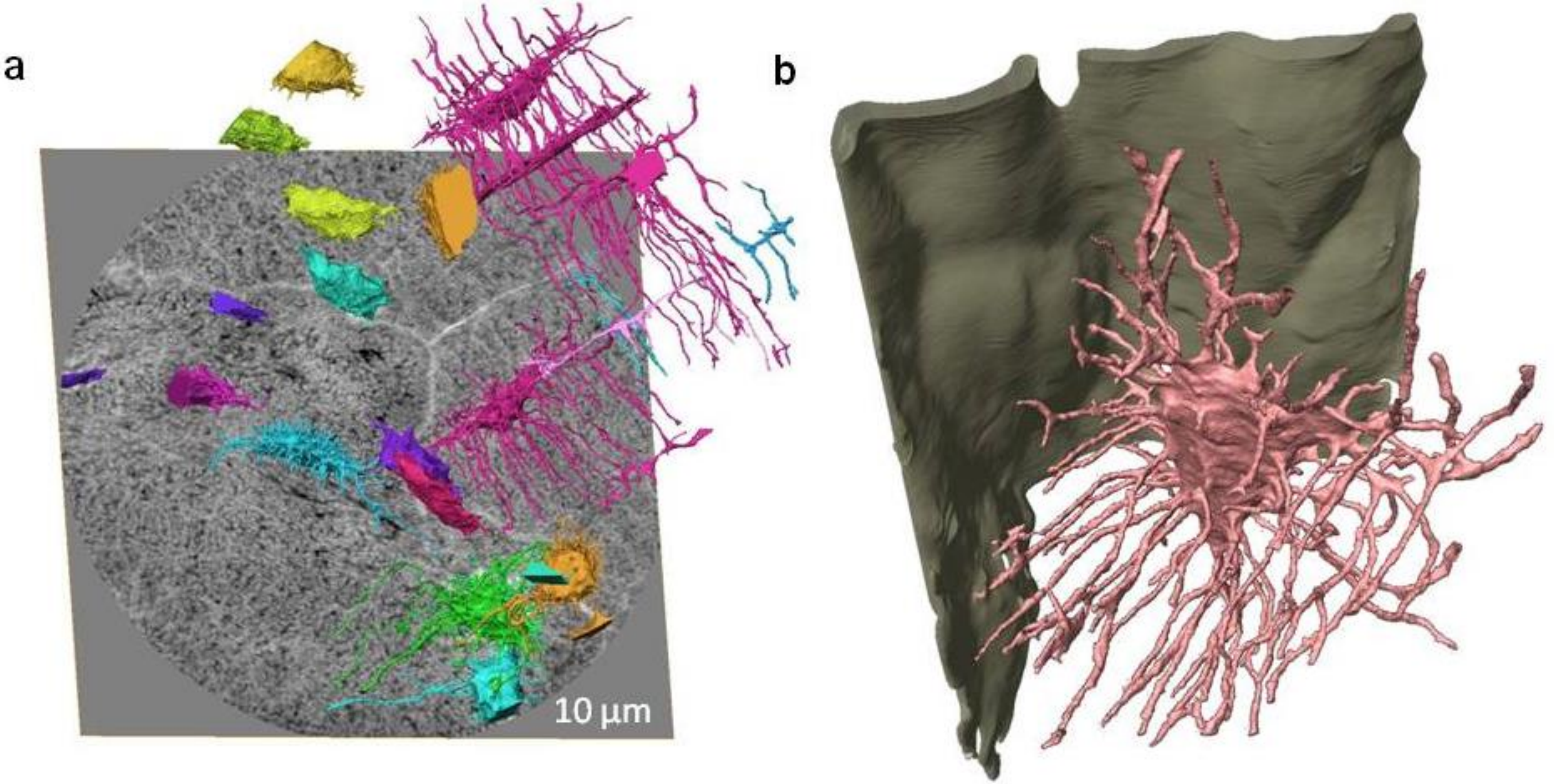

- Can easily be segmented
- 10-20 cells/volume

Phase nano-CT: application on bone

- Example on human femoral bone data

Healthy **Osteoporotic** **Osteoarthritic**

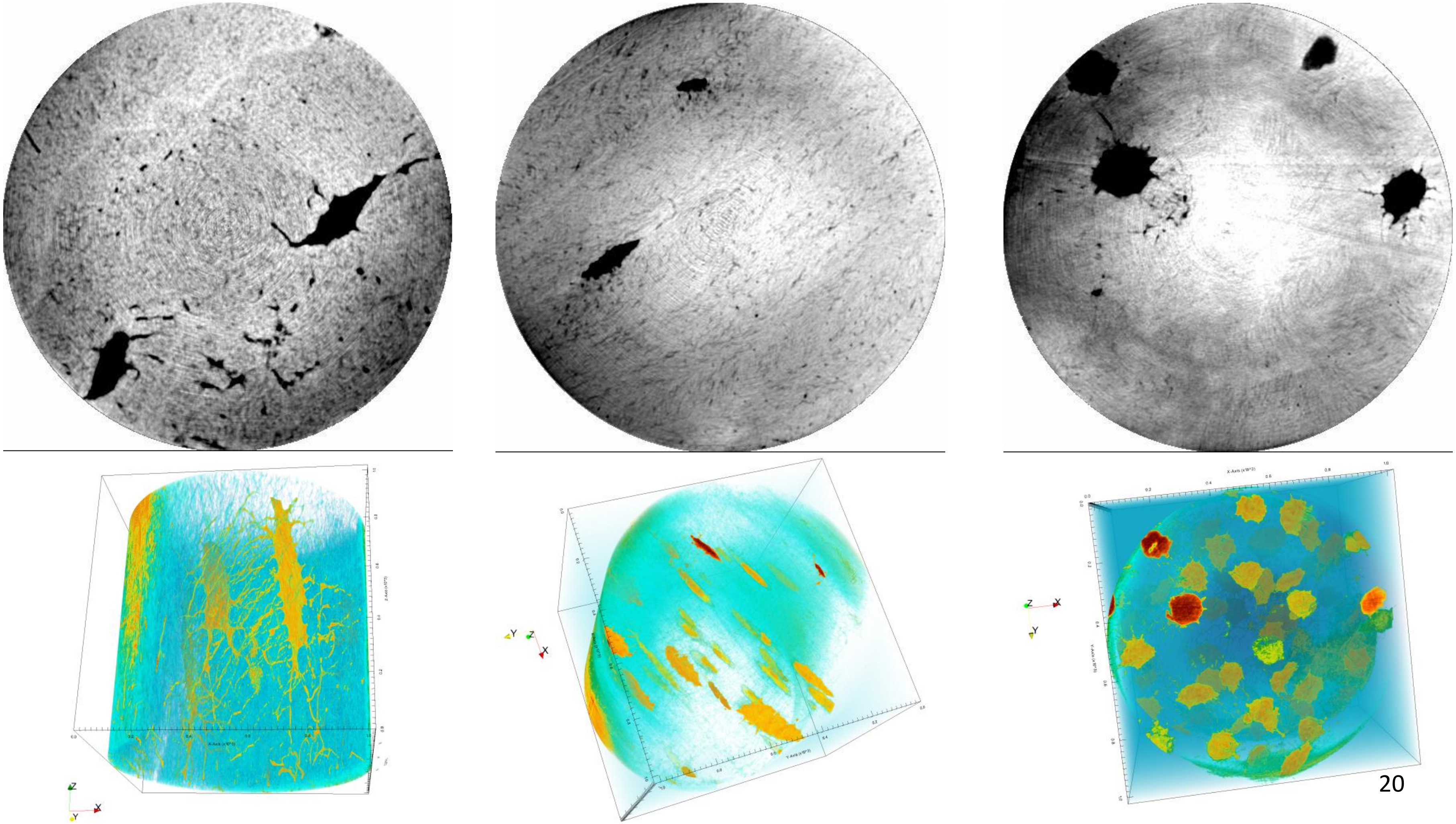

Motivation: Low frequency noise

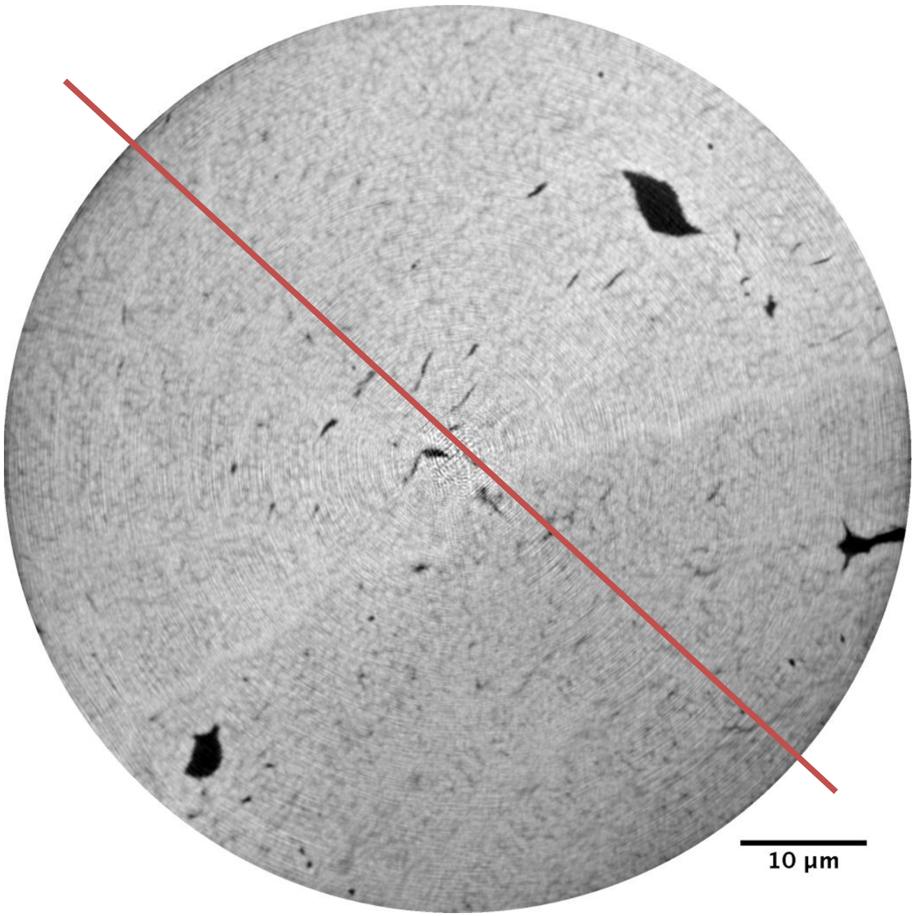

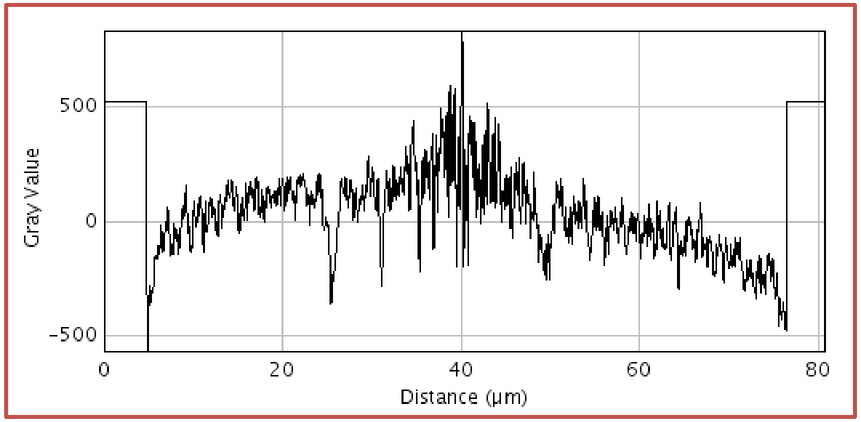

X-ray phase contrast imaging: image formation

- **Fresnel model:**

$$I_D(\mathbf{x}) = |P_D(\mathbf{x}) * u_0(\mathbf{x})|^2$$

- **First order terms** [8]:
  Linearized with respect to the object

$$\tilde{I}_D(\mathbf{f}) = \delta_{Dirac}(\mathbf{f}) - 2\cos(\pi\lambda D|\mathbf{f}|^2)\,\tilde{B}(\mathbf{f}) + 2\sin(\pi\lambda D|\mathbf{f}|^2)\tilde{\varphi}(\mathbf{f})$$

  - slowly-varying phase
  - weak attenuation

- Problem:

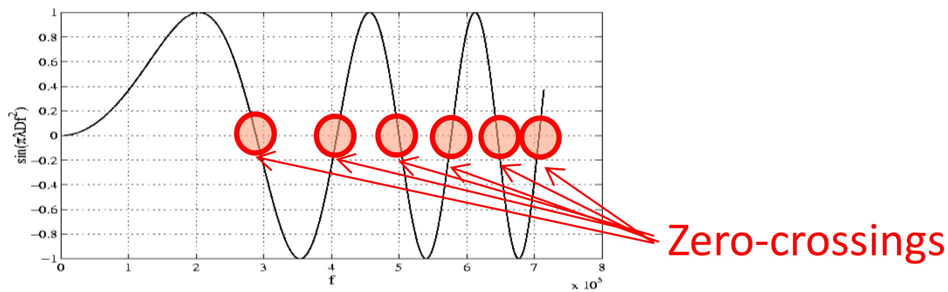

→ **Combine several distances ('holotomography')** [8, 9]

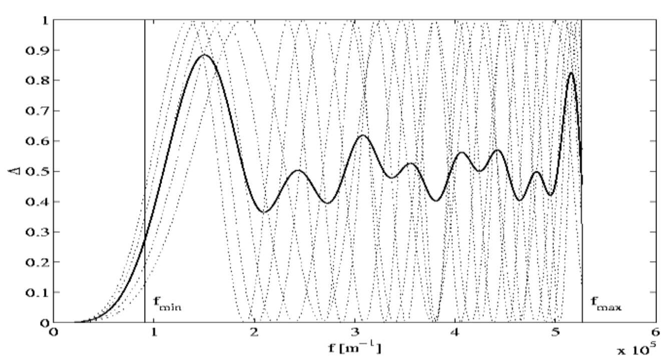

[8] Cloetens et al., *Appl. Phys. Lett.*, 1999.
[9] Zabler et al., *Rev. Sci. Inst.*, 2005

Motivation: Low frequency noise

- **Problem:** transfer function goes to 0 in the low frequencies

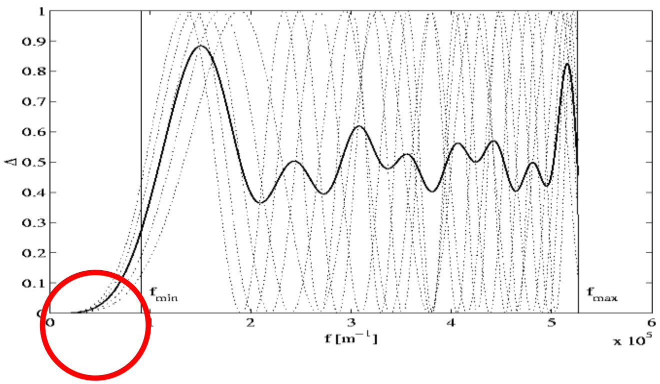

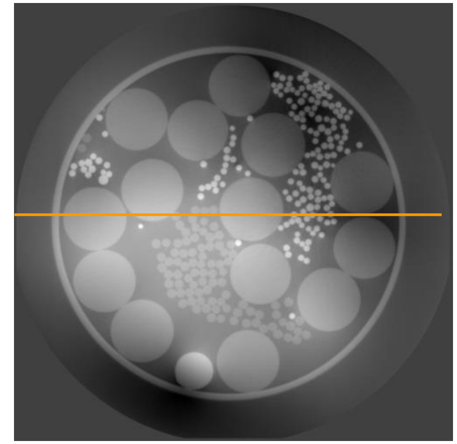

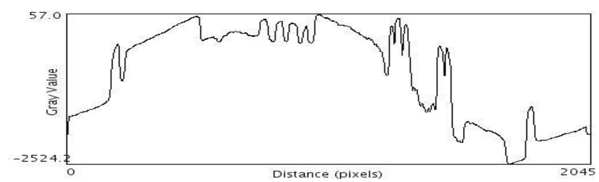

- **Motivation**
  - Simulation of artefacts e.g. LF noise
  - Test new reconstruction algorithms
  - Reduce need for synchrotron beam time
  - Optimize the experimental acquisition parameters

- **Previously:** Deterministic simulation
  - Wave-object interaction
  - Propagation

Simulation: Wave-object interaction

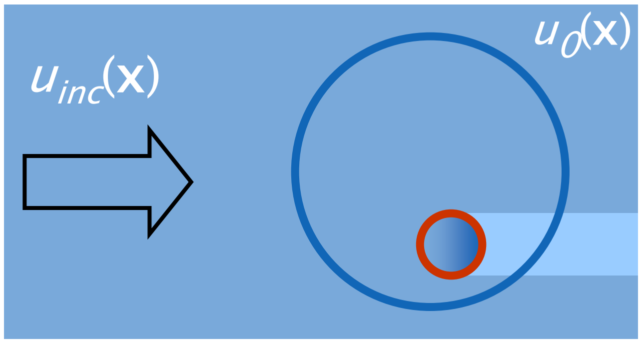

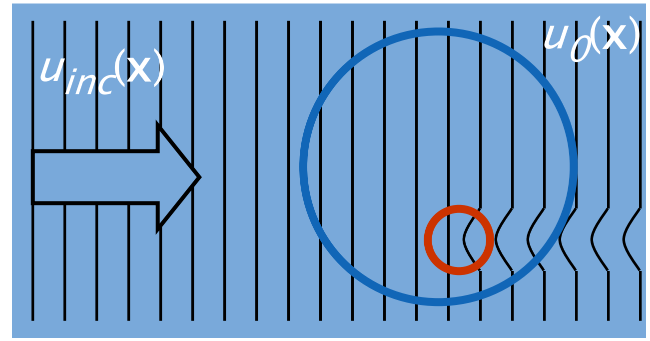

- Object described by 3D complex refractive index

$$n(x,y,z) = 1 - \delta_n(x,y,z) + i\beta(x,y,z),$$

- Wave-object interaction described by a transmittance function:

$$u_0(\mathbf{x}) = T(\mathbf{x})u_{inc}(\mathbf{x})$$

- Induces amplitude (absorption) and phase modulation:

$$T(\mathbf{x}) = A(\mathbf{x})\exp[i\varphi(\mathbf{x})] = \exp[-B(\mathbf{x})]\exp[i\varphi(\mathbf{x})].$$

- Both amplitude and phase modulation are projections through $n(\mathbf{x})$

$$B(\mathbf{x}) = \left(\frac{2\pi}{\lambda}\right)\int \beta(x,y,z)\,\mathrm{d}z \qquad \varphi(\mathbf{x}) = -\left(\frac{2\pi}{\lambda}\right)\int \delta_n(x,y,z)\,\mathrm{d}z$$

Simulation: Propagation

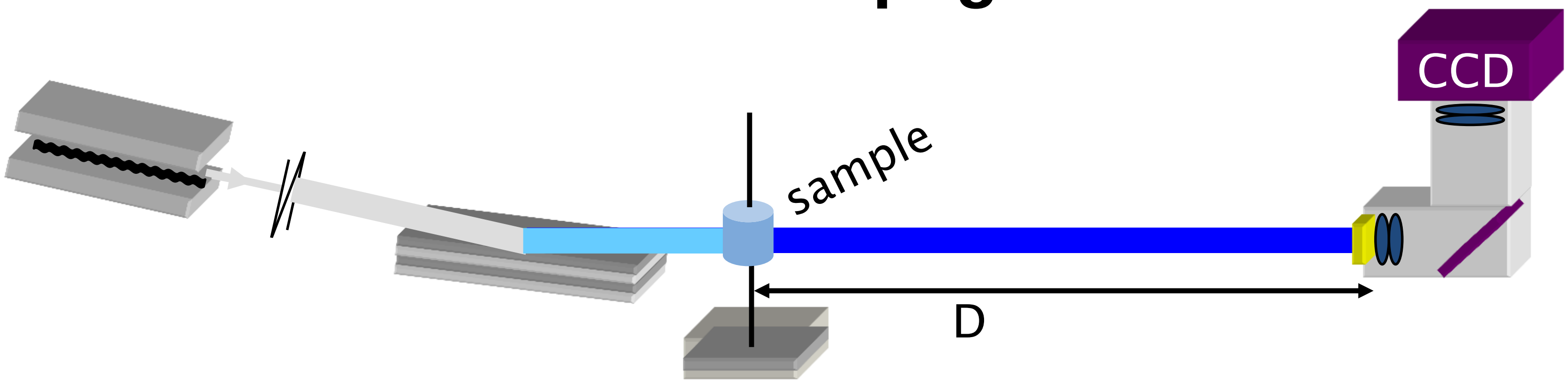

- Propagation over finite D is described by Fresnel diffraction
- Propagation is a linear system w.r.t. the wave
- Convolution of wave with propagator

$$u_D(\mathbf{x}) = P_D(\mathbf{x}) * u_0(\mathbf{x}) \qquad P_D(\mathbf{x}) = \frac{1}{i\lambda D} \exp\left(\mathrm{i}\frac{\pi}{\lambda D}|\mathbf{x}|^2\right)$$

- Fourier domain: Multiplication with propagator

$$\tilde{P}_D(\mathbf{f}) = \exp(-\mathrm{i}\pi\lambda D|\mathbf{f}|^2)$$

- Non-linear w.r.t intensity: squared modulus of wave:

$$I_D(\mathbf{x}) = |u_D(\mathbf{x})|^2,$$

- Quantitative relationship phase -> contrast

In-line phase contrast simulation tool on VIP

- Implementation on the Virtual Imaging Platform (VIP, Creatis, Villeurbanne), an imaging simulation platform [27]
    - MRI
    - PET
    - X-rays
    - Ultrasounds

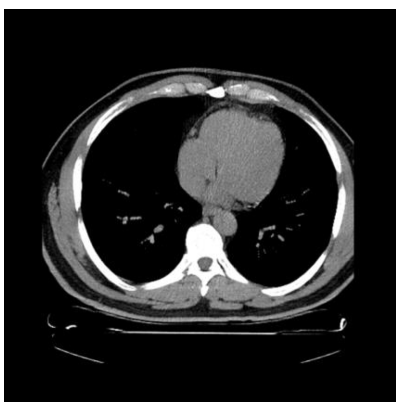

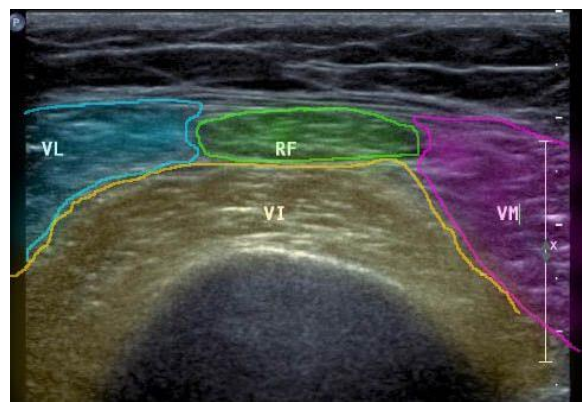

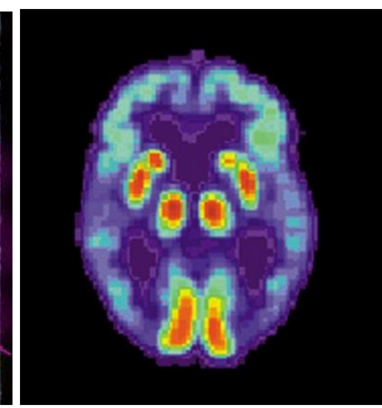

[27] Glatard *et. al*, *IEEE Trans. Med. Im.*, 2013. – **http://vip.creatis.insa-lyon.fr**

In-line phase contrast simulation tool on VIP

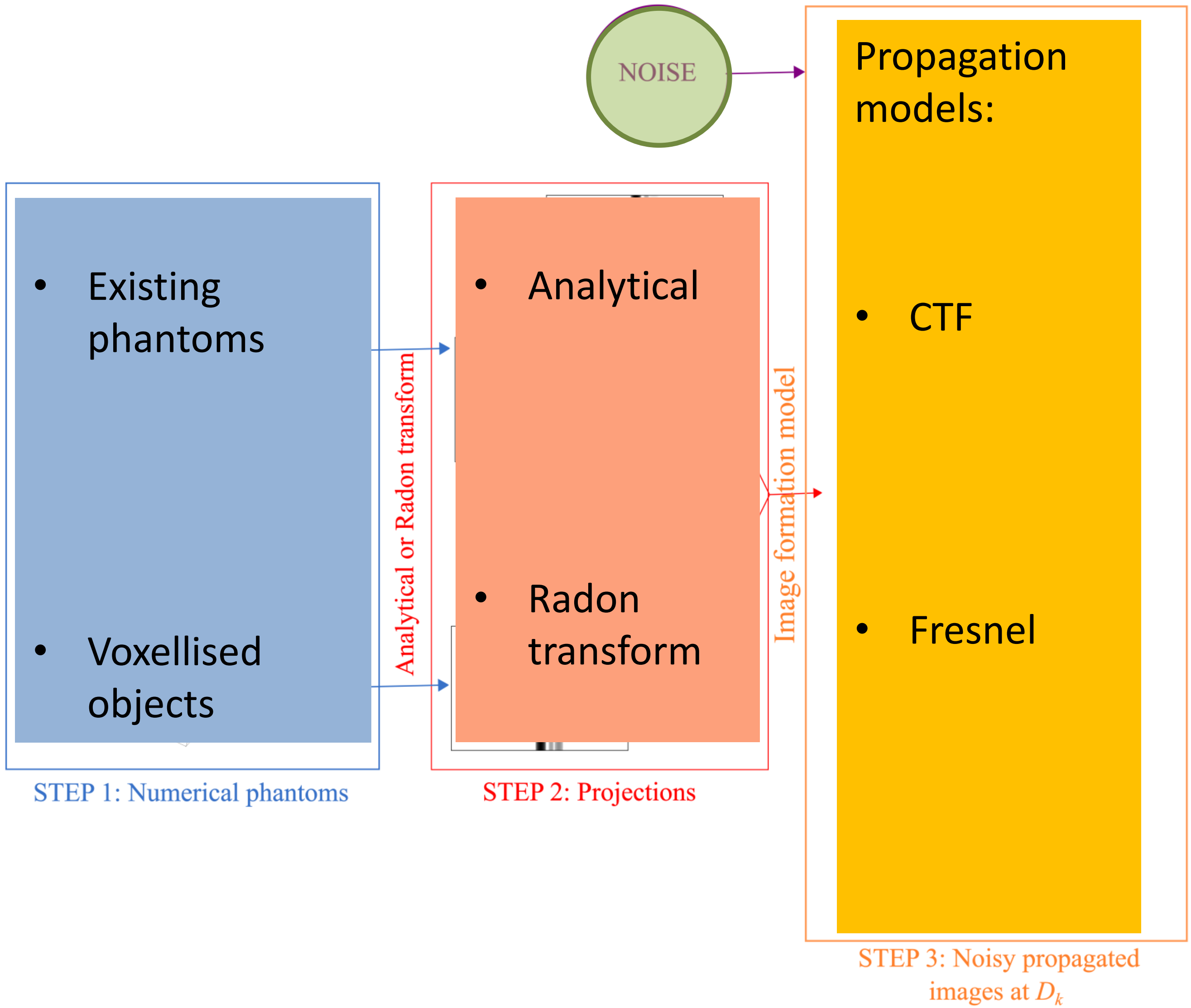

Deterministic simulation: results

- LF noise not recreated
- Hypothesis: due to scattered radiation
  - Can be simulated using Monte Carlo
  - But…
- Diffraction is a wave phenomenon, scattering is a particle phenomenon

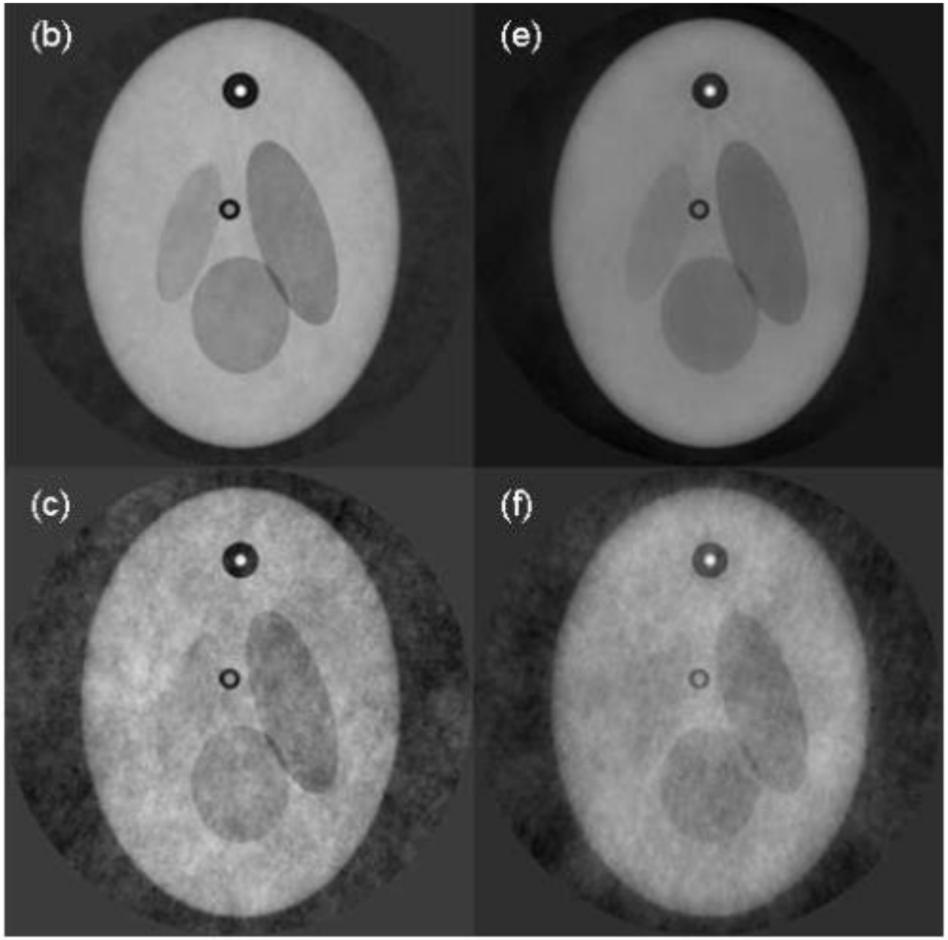

Ray optical approach

- Not straight-forward to combine diffraction and scattering

- What can we implement using standard Monte Carlo?
  - MSc Zhenjie Cen

- Refraction
- Reflection

- Implemented in Geant4

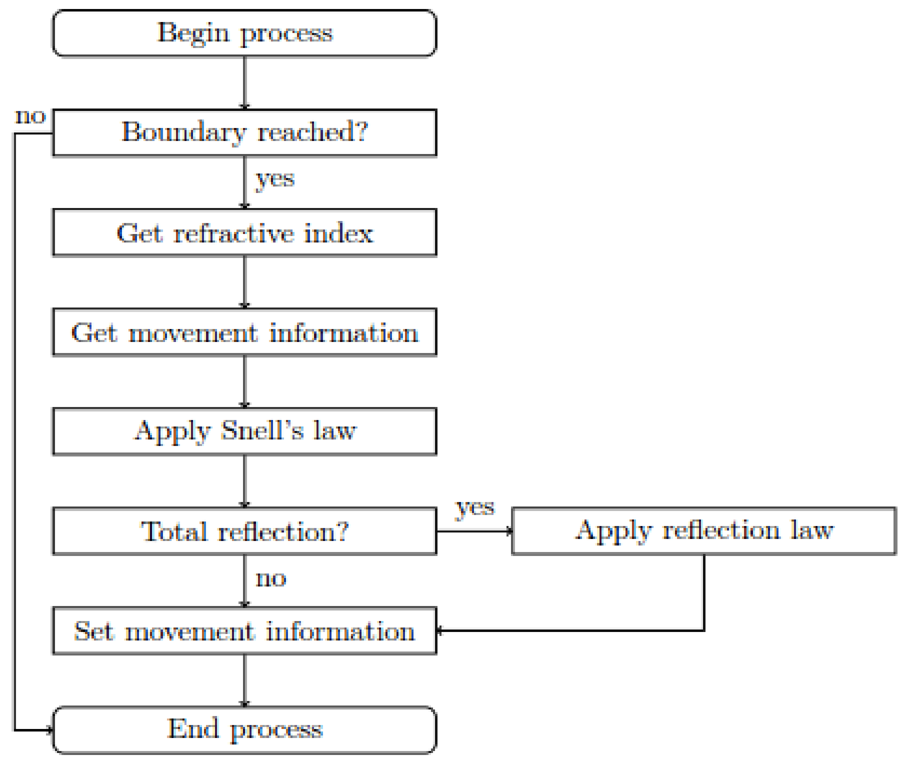

FIGURE 3.1: A schematic of the XrayBoundary process.

Deterministic process on each ray

Ray optics: example

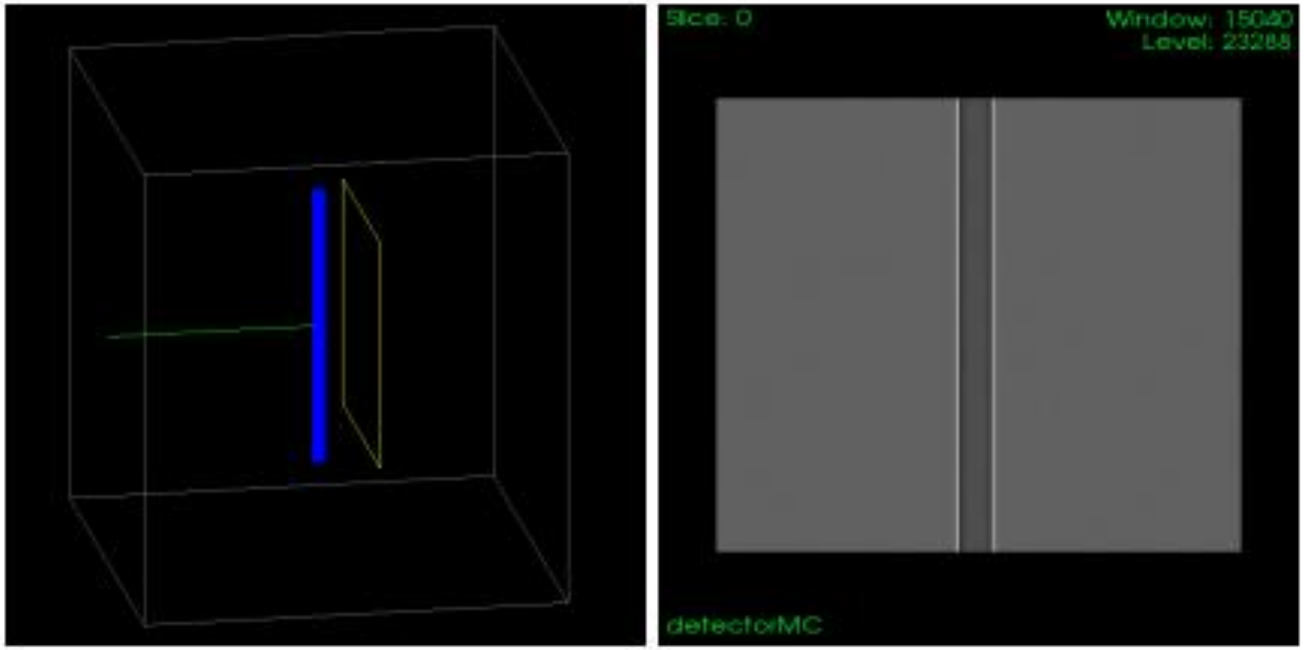

(a) Simulation setup (b) Imaged phantom

FIGURE 3.7: The phantom is an aluminium wire (blue) which has a radius of 15.208 µm. The refractive index decrement of aluminium at 19 keV is $\delta = 2.0 \times 10^{-6}$. To capture the image, we use a flat panel detector (yellow) with a pixel size of 1 µm. For the sake of simplicity, only one photon's mouvement is showed (green).

Wave optical approach

- Implemented in GATE (for comparison)
- Uses ITK for computations

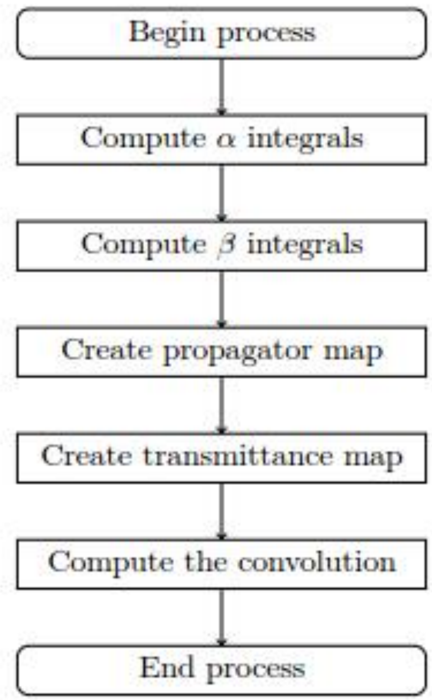

FIGURE 3.2: A schematic of the Fresnel diffraction actor algorithm.

Comparison ray/wave optical approaches

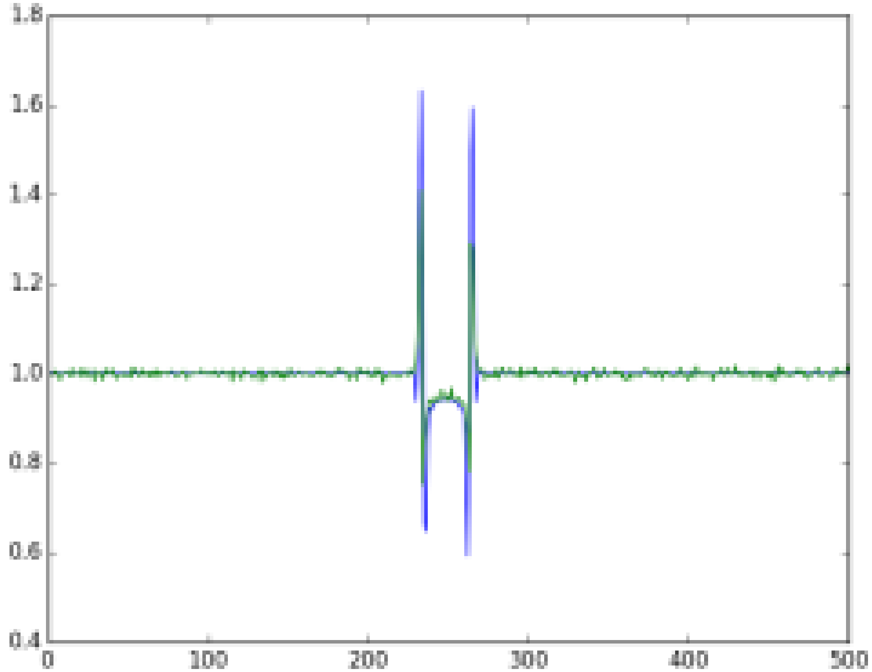

FIGURE 3.8: Comparison of the profiles of the stochastic model and the analytical model. The green curve is obtained using the Monte Carlo refraction model. The blue curve is obtained using the analytical Fresnel diffraction model

Perspectives: refraction on voxellised phantoms

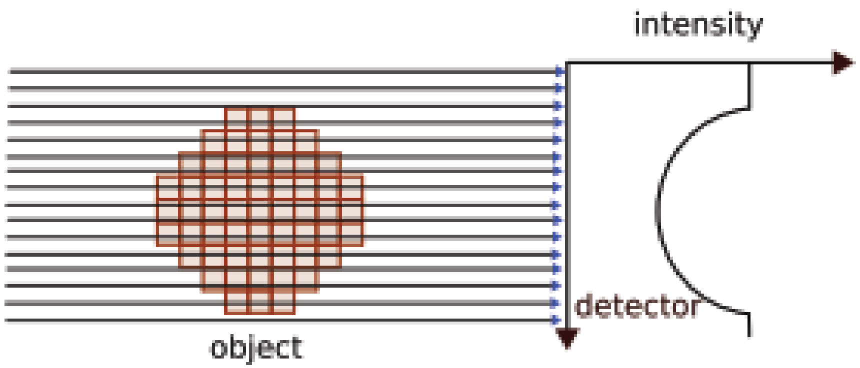

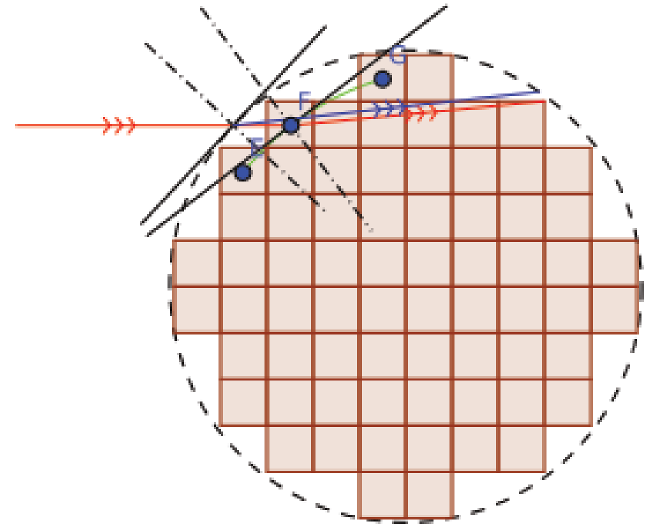

FIGURE 4.4: Schematic of the local envelope solution.

- Refraction currently limited to analytical phantoms
- Extension to voxellised phantoms
  - Calculation of refractive index gradients

Perspectives: combine wave and particle effects

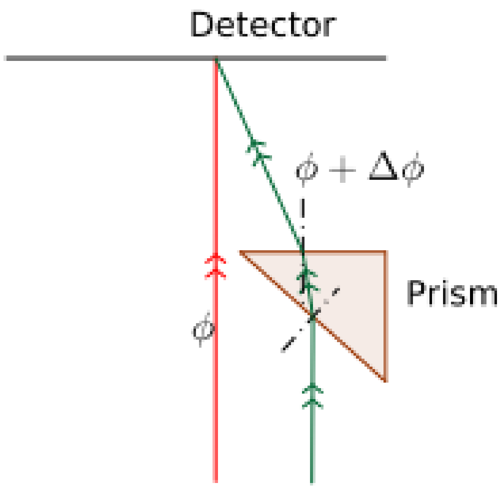

$$W(\mathbf{x},\mathbf{p}) = u_0(\mathbf{x}+\mathbf{y}/2)u_0{}^*(\mathbf{x}-\mathbf{y}/2)e^{-i\mathbf{p}\cdot\mathbf{y}}\mathrm{d}\mathbf{y}$$

- Phase as optical path length of each ray
  - Propagate with Fresnel propagator

- Sample Wigner distribution as initialisation of MC simulation
  - Phase and absorption as line integrals
  - Sample *W* for initial position **x** and momentum **p** of photons
  - Scattering and propagation in MC

Conclusions

- Simulation of X-ray phase contrast imaging

- Wave-optical approach implemented in VIP and GATE
- Ray-optical refraction approach implemented in GEANT4
- Available through VIP and GATELab
- Uses EGI

- Perspectives: Unify wave and ray optical approaches

Acknowledgments

- **Creatis**

  Loriane Weber, Françoise Peyrin,

  Cécile Olivier, Pierre-Jean Gouttenoire,
  Sorina Pop, Zhenjie Cen, Simon Rit,

  Jean Michel Letang
- **Charité, Berlin**

  Kay Raum, Peter Varga
- **LIB, Paris**

  Quentin Grimal,

  Pascal Laugier
- **ESRF**

  Bernhard Hesse, Lukas Helfen,
  Elodie Boller

  ID16
- **Labex PRIMES**
- **You for your attention and questions!**

Simulation of X-ray in-line phase contrast

M. Langer, Z. Cen, L. Weber, J. M. Letang, S. Rit, F. Peyrin

Université de Lyon, CREATIS ; CNRS UMR 5220 ; Inserm U1044 ;
INSA-Lyon ; Université Lyon 1, Villeurbanne, France.

European Synchrotron Radiation Facility, Grenoble, France

max.langer@creatis.insa-lyon.fr